Catalytic Phosphorylation of Na,K-ATPase Drives the Outward Movement of Its Cation-Binding H5−H6 Hairpin†

Lyudmila Mikhailova, Atin K. Mandal, and José M. Argüello*

Department of Chemistry and Biochemistry, Worcester Polytechnic Institute, Worcester, Massachusetts 01609

Received February 22, 2002; Revised Manuscript Received April 25, 2002

ABSTRACT: The Na,K-ATPase undergoes conformational transitions during its catalytic cycle that mediate energy transduction between the phosphorylation and cation-binding sites. Structure−function studies have shown that transmembrane segments H5 and H6 in the α subunit of the enzyme participate in cation binding and transport. The Ca-ATPase crystal structure indicates that the H5 helix extends into the cytoplasmic ATP binding domain, finishing 4−5 Å from the phosphorylation site. Here, we test whether the phosphorylation of the Na,K-ATPase leads to conformational changes in the cation-binding H5−H6 hairpin. Using as background an enzyme where all wild-type Cys in the transmembrane region were replaced, Cys were introduced in the joining loop and extracellular ends of H5 and H6. Mutated proteins were expressed in COS cells and probed with Hg^{2+}, [2-(trimethylammonium)ethyl]methanethiosulfonate (MTSET), and biotin-maleimide, applied to the extracellular media while placing the cells in two different media (*K-medium* and *Na-medium*). We assumed that under these treatment conditions most of the enzyme would be in one of two predominant conformations: E1 (*K-medium*) and E2P (*Na-medium*). The extent of enzyme inactivation by Hg^{2+} or MTSET treatment was dependent on the targeted position; i.e., proteins carrying Cys in the outermost positions were more affected by treatment. Moreover, in the case of proteins carrying Cys at positions 785, 787, and 797, driving the enzyme to phosphorylated conformations (Na-media) led to a larger inactivation. Similarly, biotinylation of introduced Cys was also influenced by the enzyme conformation, with a larger extent of modification after treatment of cells in the *Na-medium* (E2P form). These results can be explained by the enzyme phosphorylation driving the outward movement of the H5 helix. Thus, they provide experimental evidence for a structure−function mechanism where, via H5, enzyme phosphorylation leads to a conformational change at the cation-binding site and the consequent cation translocation.

The Na,K-ATPase transports Na^+ and K^+ against their concentration gradients, across the plasma membrane of animal cells (*2*). Its catalytic cycle is characterized by the formation of a phosphorylated intermediate and conformational transitions (E1→E1P→E2P→E2→E1) (*2*−*4*). These are critical for the energy transduction between the phosphorylation and the cation-binding regions of the protein. Structure−function studies have contributed to establish the location of cation- and ATP-binding sites [see, for example, (*5*−*10*)]. The ATP-binding domain is located in the large cytoplasmic loop of the α subunit, between the H4 and H5 transmembrane segments (TMs),[1] while cation-binding sites are constituted by residues in TMs H4, H5, and H6. The recently determined crystal structure of the sarcoplasmic reticulum (SR) Ca-ATPase supports the ideas generated by structure−function studies concerning the location of cation- and nucleotide-binding sites (*11*). Furthermore, it provides a structural base to develop a functional model. Figure 1 shows a diagram of the Na,K-ATPase α subunit constructed by homology modeling based on the Ca-ATPase crystal structure (PDB 1EUL).[2] Sweadner and Donnet, using comparable modeling methods, have described the similarities of these two enzymes and the consequent validity of this modeling approach as a tool for proposing testable hypotheses (*12*).

The Na,K-ATPase α subunit model indicates that approximately 50 Å separates the phosphorylation and cation-binding sites. This is a significant distance considering the necessary communication between these two sites and prompts the question of how the long-distance interaction is mediated. It was earlier proposed that key conformational changes are transmitted between the phosphorylation and the cation-binding sites via the stalk region of the enzyme constituted by extensions of TMs H2, H3, H4, and H5 (Figure 1) (*13*). Several laboratories have explored the putative role of this region in energy transduction in different

† This work was supported by Grant-in-Aid 9750102N from the American Heart Association.

* To whom correspondence should be addressed. Phone: (508) 831-5326, Fax: (508) 831-5933, E-mail: arguello@wpi.edu.

[1] Abbreviations: DEAC, 4-(diazomethyl)-7-(diethylamino)-coumarin; HRP, horseradish peroxidase; MTSET, [2-(trimethylammonium)ethyl]-methanethiosulfonate; SR, sarcoplasmic reticulum; TMs, transmembrane segments.

[2] All amino acid positions refer to the sheep α1 subunit sequence (*1*). Numbering of this sequence does not include five residues in the leader sequence.

10.1021/bi025721k CCC: $22.00
Published on Web 05/25/2002

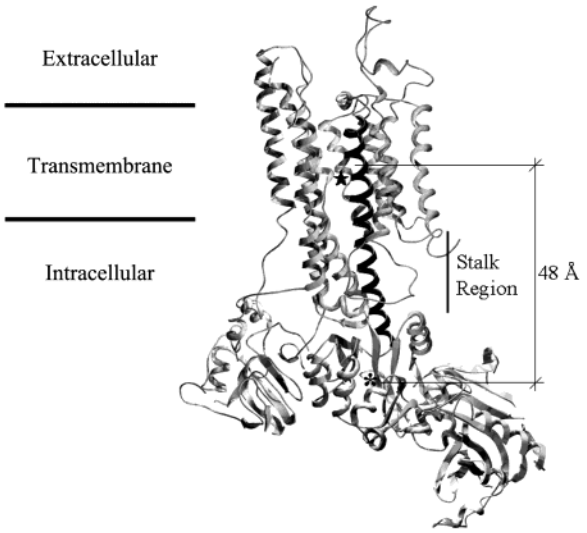

FIGURE 1: Na,K-ATPase α subunit. The homology model is based on the SR Ca-ATPase structure (PBD 1EUL). Gaps in the structure reflect fragments not present in the Na,K-ATPase sequence.[2] (∗) Phosphorylation site, Asp369. (★) Cation binding, located among Asp^{804}, Asp^{808}, Glu^{779}, Ser^{775}, Glu^{327}. H5 extending from Phe^{748} until I^{788} is in black.

P-type ATPases (*14*−*17*). However, analysis of the Ca-ATPase structure and the Na,K-ATPase model suggests a quite simple link between the phosphorylation and cation-binding sites via a long central helical structure. This helix includes the 5th TM (H5) and its extension into the stalk region (S5) (black in Figure 1) (*18*). The Na,K-ATPase H5−S5 helix starts at Phe^{748}, only 4−5 Å from the phosphorylation site, and, extending into the transmembrane region, probably provides at least two amino acid side chains (Ser^{775} and Glu^{779}) to the cation-binding sites (*8*−*10*, *19*). Contrary to H4 and H6, that also contribute residues to cation-binding sites (*20*, *21*), H5 does not present a kink and appears to be a rather rigid structure that might transmit movement. Movement or displacement of H5 with respect to other TMs is suggested by the faster modification of Glu^{779} by 4-(diazomethyl)-7-(diethylamino)-coumarin (DEAC) when the enzyme is placed in a phosphorylated conformation (*10*, *22*). Furthermore, after proteolytic cleavage, the H5−H6 hairpin is released from the membrane as an apparently soluble fragment, suggesting a weak interaction with neighboring TMs and its possible mobility within the transmembrane structure of the protein (*23*, *24*). The functional mobility of H5 might also play a role in the mechanism for enzyme inactivation by ouabain since residues in the H5−H6 hairpin are associated with binding of the steroid (*25*, *26*). Thus, diverse lines of evidence suggest a hypothetical mechanism where the enzyme phosphorylation would drive the movement of the H5 helix, leading to a local conformational change at the cation-binding site and a consequent change in cation affinity.

We present here experimental evidence supporting the role of H5 as a key link between enzyme phosphorylation and cation-binding sites. We assumed that structural changes due to enzyme phosphorylation are transmitted along H5 and could be detected by accessibility changes in amino acids at the extracellular loop of the H5−H6 hairpin. Using as a background a Na,K-ATPase α subunit devoid of Cys in the transmembrane region (All-TM-Cys), Cys were introduced

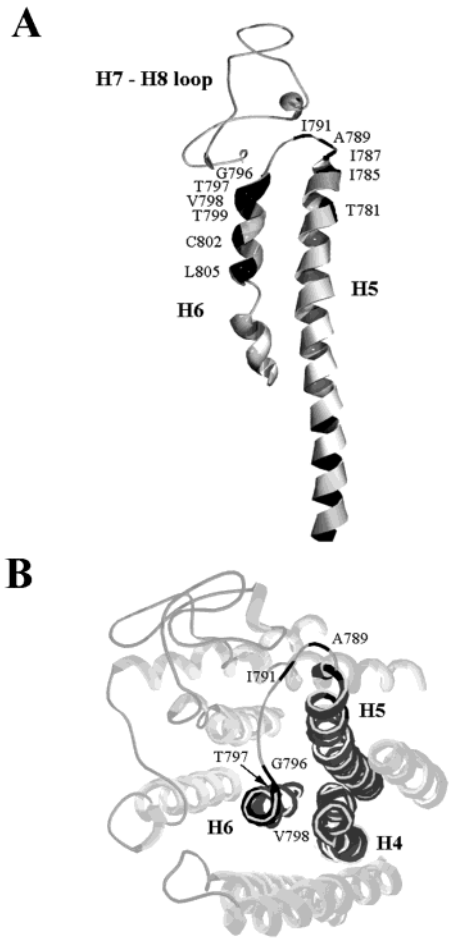

FIGURE 2: Detail of the α subunit H5 and H6 transmembrane segments. (A) Model shows the H5−H6 hairpin, the extended H5 helix, and the closely located H7−H8 joining loop. The locations (in black) of residues substituted by Cys are indicated. (B) Extracellular side view of all TMs and joining loops. H4, H5, and H6 are in black.

in the extracellular ends of H5 and H6 and their joining loop. The movement of this region was established by the differential reactivity of the introduced Cys with extracellularly applied reagents while placing the enzyme in phosphorylated and dephosphorylated conformations.

EXPERIMENTAL PROCEDURES

Site-Directed Mutagenesis. The eukaryote expression vector pKC4 was used in these studies. This vector contains the sheep Na,K-ATPase α1 subunit cDNA modified to encode for the $Gln^{111}Arg$ and $Asn^{122}Asp$ replacements, yielding a form of the enzyme with low affinity for ouabain (RD) (*27*). A construct encoding a RD α subunit void of endogenous transmembrane cysteines was used as a template for mutagenesis (it carries replacements $Cys^{104,138,964}Ser$, $Cys^{336,802,911,930,983}Ala$ and is referred to in this work as All-TM-Cys) (*28*, *29*). Site-directed mutagenesis was performed either with the "mega-primer" method (*30*) or with the Quick change site-directed mutagenesis kit (Stratagene, La Jolla, CA). Nucleotide substitutions were made to introduce single Cys replacements of each amino acid in the sequence T^{781}PFLIFIIANIPLPLGTVTILCIDL^{805} (see Figure 2). In the case of Cys^{802}, Cys was reintroduced within the background of the All-TM-Cys construct. Each mutant was verified by

automatic DNA sequencing. To perform experiments requiring affinity purification of the heterologously expressed proteins, a $(His)_6$-tag encoding sequence was introduced into the 5′ end of the corresponding cDNAs. COS cells were transfected with these vectors using Lipofectamine 2000 (Invitrogen, Carlsbad, CA) and selected by inclusion of 1 μM ouabain in the culture medium. Ouabain-resistant colonies were isolated and expanded into stable cell lines. COS cells were maintained in Dulbecco's modified Eagle media, 10% calf serum, supplemented with 20 mM KCl (*8*), at 37 °C in humidified air at 5% CO_2.

Membrane Preparation and Enzyme Activity Assays. Crude membranes from COS cells were prepared using NaI treatment (*31*). All protein determinations were performed in accordance with Bradford (*32*) using bovine serum albumin as standard.

The Na,K-ATPase activity was measured as previously described (*8*). The Na,K-ATPase corresponding to expressed protein was calculated by subtracting the activity observed in the presence of 10 mM ouabain (inhibits both the endogenous and the heterologously expressed enzymes) from that detected with 0.01 mM ouabain (which inhibits only the endogenous enzyme). The apparent cation affinities were estimated as the $K_{1/2}$ for ATPase activation, fitting activity versus [cation] curves to the equation: $v = V_{max}L^n/(L^n + K_{1/2})$, where L is the cation concentration and $n = 2$ for K^+ and $n = 3$ for Na^+. The K_m of ATP at the low-affinity site was calculated from activity versus [ATP] curves fitted to simple Michaelis kinetics.

Treatment of Intact Cells Expressing Cysteine-Substituted Enzymes with Hg^{2+}, [2-(Trimethylammonium)ethyl]-methanethiosulfonate (MTSET), or Biotin-maleimide. COS cells expressing the heterologous proteins were grown in 24 well plates. Cells were rinsed with (mM) 60, NaCl; 100, choline-Cl; 5, glucose; 0.5, $MgCl_2$; 4, P_i-Tris, pH 7.4 (Solution A), and then treated in two different systems that differ in Na^+ and K^+ compositions (*28*). All procedures were performed at room temperature (20−22 °C). "*Na-medium*": The cells were preincubated for 5 min in a solution containing (mM) 5, NaCl; 135, choline-Cl; 5, glucose; 0.5, $MgCl_2$; 4, P_i-Tris, pH 7.4; 0.01, bumetanide; 0.012, monensin; and either 0.001 or 2, ouabain. After preincubation, the cells were treated in this medium plus 10 μM $HgCl_2$, 5 mM MTSET (Toronto Res. Chem., North York, Ontario), or 0.5 mM biotin-maleimide (Molecular Probes, Eugene, OR), for 30 s, 30 s, or 30 min, respectively. "*K-medium*": The cells were preincubated for 5 min in a solution containing (mM) 5, KCl; 135, choline-Cl; 5, glucose; 0.5, $MgCl_2$; 4, P_i-Tris, pH 7.4; 0.01, bumetanide; 0.012, monensin; and either 0.001 or 2, ouabain. Following preincubation, the cells were treated with $HgCl_2$, MTSET, or biotin-maleimide as indicated above. K^+ transport assays or biotinylation detection procedures were subsequently initiated (see below).

K^+ Transport Assay. K^+ uptake into COS cells, using $^{86}Rb^+$ as congener, was measured as described by Munzer et al. (*33*). After treatment under different conditions (either *Na-medium* or *K-medium*), cells were rinsed and incubated 5 min in Solution A plus (mM) 5, KCl; 0.01, bumetanide; 0.012, monensin; and either 0.001 or 2, ouabain. Uptake was initiated by replacing the washing media with Solution A plus (mM) 1.5, KCl; $^{86}Rb^+$ (0.5 μCi); 0.01, bumetanide; 0.012, monensin; and either 0.001 or 2, ouabain. The assay was performed at 37 °C for 10 min and ended by removing the media and washing the cells with ice-cold Solution A. The cells were solubilized with 0.2 M NaOH, and aliquots were taken for protein and radioactivity quantification in a scintillation counter. K^+ uptake corresponding to expressed protein was calculated by subtracting the uptake observed in the presence of 2 mM ouabain (inhibits both the endogenous and the heterologously expressed enzymes) from that measured in the presence of 0.001 mM ouabain (inhibits the endogenous enzyme). Background uptake measured in the presence of 2 mM ouabain was not modified by Hg^{2+} or MTSET treatment.

Detection of Biotinylated Heterologous Na,K-ATPase α Subunit. COS cells expressing $(His)_6$-tagged mutants were used for these experiments. Cells were rinsed twice with Solution A, preincubated in either "*Na-medium*" or "*K-medium*", and treated with biotin-maleimide as indicated above. After treatment, cells were rinsed twice with solution A and resuspended with a cell lysis buffer: 50 mM Tris, pH 7.4, 100 mM NaCl, 50 mM NaF, 10 mM sodium pyrophosphate, 200 μM Na_3VO_4, 1% $C_{12}E_8$, and a protease inhibitor cocktail (100 μg/mL phenylmethylsulfonyl fluoride; 1 μg/mL each of leupeptin, aprotinin, pepstatin A, and soybean trypsin inhibitor). The expressed proteins were then subjected to immunoprecipitation using anti-His-tag antibody and Protein A-Agarose (Santa-Cruz Biotechnology, Santa Cruz, CA) as described by Efendiev et al. (*34*). After immunoprecipitation, samples were separated by SDS−polyacrylamide gel electrophoresis using 7.5% tricine gels (*35*), and proteins were blotted onto a nitrocellulose membrane. The heterologous Na,K-ATPase α subunit was detected with monoclonal anti-sheep α subunit antibody (Affinity Bioreagents, Golden, CO). Biotinylated protein bands were detected with horseradish peroxidase (HRP)-conjugated streptavidin (Molecular Probes, Eugene, OR).

Molecular Modeling. The homology modeling of the Na,K-ATPase α subunit using the SERCA1a structure file, PDB 1EUL, was done with Swiss PDB viewer software (*36*) (http://expasy.cbr.nrc.ca/spdbv). Final rendering of the figures was done with POVray software (http://www.povray.org).

RESULTS

Cysteine Mutagenesis of Residues in the H5−H6 Hairpin. Functional Characterization of Cysteine-Substituted Enzymes. The goal of these experiment was to test the putative role of the H5 helix in transmitting the conformational changes between the phosphorylation and cation-binding sites of the Na,K-ATPase. We hypothesized that as a consequence of this structural−functional link the accessibility of amino acids in the joining loop and extracellular ends of H5 and H6 would be affected by enzyme phosphorylation/dephosphorylation. To examine these changes in accessibility, amino acids in this region were replaced with Cys in the background of an enzyme lacking endogenous transmembrane Cys. The resulting proteins were expressed in COS cells and probed (in intact cells) with Cys-specific reagents applied to the extracellular media.

We focus our attention on those H5−H6 residues likely to be accessible to treatment with extracellular applied probes, i.e., amino acids in the joining loop and most external helix turns. To identify the amino acids in this region, the

Table 1: Enzymatic Characterization of Cysteine-Substituted Enzymes

construct	Na,K-ATPase[a] (μmol mg^{-1} h^{-1})	K^+ uptake[b] (nmol mg^{-1} h^{-1})	K_m(ATP) (mM)	$K_{1/2}$(Na^+) (mM)	$K_{1/2}$(K^+) (mM)
RD	77.8 ± 3.5	93.6 ± 10.5	0.47 ± 0.11	3.99 ± 0.38	0.21 ± 0.07
All-TM-Cys	33.7 ± 5.6	63.5 ± 6.7	0.43 ± 0.08	5.14 ± 0.31	0.09 ± 0.07
Thr^{781}Cys	29.9 ± 1.5	40.2 ± 5.6	0.43 ± 0.11	7.17 ± 0.58	0.39 ± 0.06
Ile^{785}Cys	45.7 ± 8.4	65.3 ± 6.0	0.40 ± 0.13	4.16 ± 0.47	0.82 ± 0.14
Ile^{787}Cys	31.8 ± 4.5	19.5 ± 0.9	0.20 ± 0.05	2.64 ± 0.19	1.19 ± 0.39
Ala^{789}Cys	67.1 ± 7.8	32.5 ± 3.1	0.20 ± 0.05	4.74 ± 0.26	0.73 ± 0.15
Ile^{791}Cys	29.0 ± 3.2	42.6 ± 1.3	0.30 ± 0.07	5.45 ± 0.57	0.34 ± 0.09
Gly^{796}Cys	25.9 ± 0.2	33.1 ± 2.8	0.51 ± 0.08	3.61 ± 0.35	0.25 ± 0.13
Thr^{797}Cys	37.7 ± 2.9	73.3 ± 10.4	0.24 ± 0.07	3.73 ± 0.73	0.32 ± 0.05
Val^{798}Cys	46.3 ± 1.6	17.2 ± 2.1	0.35 ± 0.08	3.54 ± 0.37	0.58 ± 0.12
Thr^{799}Cys	39.1 ± 1.8	140.3 ± 16.2	0.28 ± 0.03	4.58 ± 0.80	0.79 ± 0.29
Cys^{802}	40.7 ± 0.4	109.8 ± 9.5	0.37 ± 0.04	5.97 ± 0.83	0.82 ± 0.16
Leu^{805}Cys	40.9 ± 2.4	47.6 ± 7.0	0.28 ± 0.06	4.76 ± 0.82	0.42 ± 0.03

[a] ATPase activity, ATP, and cation dependence were measured in membrane preparations from COS cells expressing the indicated Cys-substituted protein. Na,K-ATPase activity is expressed as milligrams of heterologous protein. [b] K^+ uptake was measured in whole cells expressing the indicated Cys-substituted protein. K^+ uptake is expressed as milligrams of total protein.

crystal structure of the SR Ca-ATPase (PDB 1EUL) was used for modeling the Na,K-ATPase α subunit (Figures 1 and 2). Based on this model, residues in the T^{781}PFLIFIIANIPL-PLGTVTILCIDL^{805} sequence were selected to be individually replaced by Cys. Mutated proteins were expressed in COS cells under ouabain selective pressure. This system requires that the expressed ATPases be functional to maintain cell viability (a minimum of 20−25% of the rate observed for the wild-type enzyme is necessary) (*8*, *19*). Considering the multiple changes introduced in these proteins (Gln^{111}Arg, Asn^{122}Asp, Cys^{104,138,964}Ser, and Cys^{336,802,911,930,983}Ala, in addition to the Cys substitute), it was expected that some of the amino acid replacements would lead to nonfunctional enzymes. Proteins carrying Cys replacement of amino acids Pro^{782}, Phe^{783}, Leu^{784}, Phe^{786}, Ile^{788}, Apn^{790}, Pro^{792}, Leu^{793}, Pro^{794}, Leu^{795}, Ile^{800}, Leu^{801}, Ile^{803}, Asp^{804} were unable to support cell growth and consequently were not used in our studies. Cys-substituted enzymes that retained functionality and were able to support cell growth are listed in Table 1 (see Figure 2 for their location within the H5−H6 hairpin). The Na,K-ATPase activity, K^+ transport capacity, and apparent affinities of these enzymes for Na^+, K^+ and ATP were determined in order to verify that they retained functional characteristics similar to control enzymes; i.e., analogous interactions with ligands and E1↔E2 distribution. Table 1 shows that mutated enzymes, although with reduced specific activities, retained characteristics comparable to those of control proteins. No major changes in nucleotide or cation affinities were detected, except in the case of Ile^{787}Cys replacement that led to a reduced apparent affinity for K^+. Variations between different mutants in K^+ transport were associated with different expression levels. Most important, the retention of functional characteristics and the significant K^+ transport activity of all expressed proteins indicated their suitability for these studies.

Accessibility of Introduced Cysteines. We have previously described a system in which the enzyme can be placed in different conformations without disrupting cell membrane integrity and permeability to Cys reacting probes (*28*). Briefly, cells are preincubated in a "*Na-media*" where Na^+ at both sides of the plasma membrane is 5 mM and extracellular K^+ is 0 mM. We have assumed that this treatment sets the enzyme predominantly in phosphorylated forms E2P/E2P(Na) (*2*, *37*−*40*). Alternately, the cells are preincubated in "*K-media*" where intracellular Na^+ is driven close to 0 mM by extensive washing with 12 μM monensin, 0 mM external Na^+ while extracellular K^+ is kept at 5 mM. We have assumed that under this condition the enzyme is driven to dephosphorylated conformations (E2(K)/E1ATP) (*2*, *37*, *38*). These manipulations were used to set the enzyme in a phosphorylated or a dephosphorylated form while it was treated with Cys-specific reagents. Three different reagents were used, Hg^{2+}, MTSET, and biotin-maleimide, considering that not only the position of the introduced Cys but also the characteristics of the probes would influence whether the differential reactivity of the targeted residue was detected.

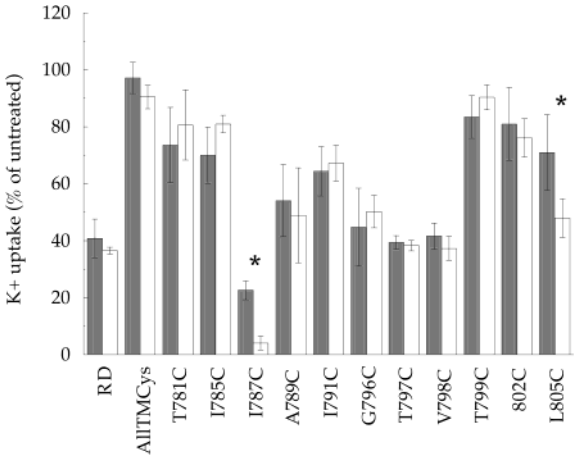

FIGURE 3: Inactivation of Cys-substituted enzymes by treatment with Hg^{2+}. K^+ uptake by the indicated enzyme was measured after treatment of whole cells with 10 μM $HgCl_2$ for 30 s in *K-medium* (gray bars) or *Na-medium* (white bars). K^+ uptake by the corresponding untreated cells was 100%. Background uptake measured in the presence of 2 mM ouabain was not modified by Hg^{2+} treatment.

Figure 3 shows the modification of the introduced Cys by Hg^{2+} as accessed by enzyme inactivation. As previously shown, the control All-TM-Cys was not affected by the Hg^{2+} treatment under our experimental conditions (*28*). Similarly, Cys introduced in deeper positions within the enzyme structure (Thr^{781}Cys, Ile^{785}Cys, Thr^{799}Cys, Cys^{802}) did not appear to react with the probe or their modification did not lead to enzyme inactivation. On the other hand, Cys residues introduced close to the extracellular loop (positions 787, 789, 791, 796, 797, and 798) were modified by the probe. Most

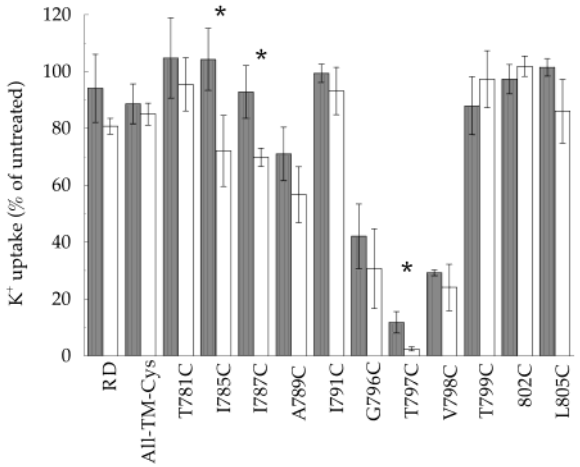

FIGURE 4: Inactivation of Cys-substituted enzymes by treatment with MTSET. K^+ uptake by the indicated enzyme was measured after treatment of whole cells with 5 mM MTSET for 30 s in *K-medium* (gray bars) or *Na-medium* (white bars). K^+ uptake by the corresponding untreated cells was 100%. Background uptake measured in the presence of 2 mM ouabain was not modified by MTSET treatment.

significantly, the modification of Ile^{787}Cys-replaced enzyme was dependent on the enzyme conformation. In this case, a larger inactivation was observed when the enzyme was treated while set in the E2P (*Na-medium*) conformation. Experiments performed with various treatments and Hg^{2+} concentrations failed to show conformation-dependent, differential reactivity of Cys introduced at other positions (not shown).

Treatment of cells expressing Cys-substituted enzymes with MTSET confirmed the pattern observed with Hg^{2+} and provided further insight into the arrangement of the H5−H6 joining loop (Figure 4). Again, Cys introduced in the joining loop (787−798) appeared more reactive, and the accessibility of Cys introduced in the extracellular turns of the H5 and H6 helixes (Thr^{785}Cys, Ile^{787}Cys, Thr^{797}Cys) was dependent on the treatment conditions. Thus, setting the enzyme in a phosphorylated conformation (*Na-medium*) during treatment led to a larger inactivation. It is interesting that the Leu^{791}Cys enzyme was not inactivated by MTSET. Although it is possible that the modification of this Cys might not affect activity, a simpler explanation is that the modification of this position is prevented by the proximity of the H7−H8 loop (Figure 2).

Increased accessibility of residues in the H5−H6 hairpin in the phosphorylated enzyme was more evident in the modification of these enzymes with the large probe biotin-maleimide (Figure 5). In this case, Cys modification was monitored by HRP−streptavidin binding to biotinylated protein after immunoprecipitation of the Cys-substituted enzymes with anti-$(His)_6$ tag antibodies. Figure 5A shows that Cys residues introduced in the outermost turn of the H5 and H6 helices (positions 787, 789, 791, 797, and 798) were differentially modified depending on the enzyme conformation. As expected, biotin-maleimide did not react with the control lacking transmembrane Cys (All-TM-Cys). This is relevant since biotin-maleimide might permeate the cell membranes; nevertheless, additional controls were performed. Figure 5B shows that proteins previously treated with the membrane-impermeable MTSET did not react with biotin-maleimide, indicating that extracellular, exposed Cys were biotinylated in these experiments.

The interaction of the enzyme with ouabain is well characterized (*41*−*43*). The phosphorylated form of the enzyme has a higher affinity for ouabain and is stabilized by inhibitor binding (*42*, *43*). The participation of residues in the H5−H6 extracellular loop (Phe^{786}, Leu^{793}, Thr^{797}) in ouabain binding has been proposed (*25*, *26*). Considering that the presence of ouabain could prevent the modification of Cys in the H5−H6 loop or lead to an increase in labeling by stabilizing the E2P form, several Cys-substituted enzymes were probed in the presence of 2 mM ouabain. The high ouabain level was necessary to bind the sheep RD α subunit used in these studies (*27*). Figure 5C shows that, as expected, the presence of ouabain reduced the labeling of Thr^{797}Cys-substituted enzyme. This effect was even clearer in the case of the enzyme mutated in the neighboring position, Val^{798}Cys. As a control, modification of Ala^{789}Cys or Gly^{796}Cys replaced enzymes was not prevented by the steroid. Moreover, ouabain increased the labeling of Gly^{796}Cys, likely by stabilizing the E2P form.

DISCUSSION

P-type ATPases couple ion transport to ATP hydrolysis. Here, we examined the hypothesis that in the Na,K-ATPase the required energy transduction between phosphorylation and cation transport is mediated by the long H5 helix. Our results indicate that upon enzyme phosphorylation there is an increase in exposure of the H5−H6 hairpin to extracellular probes, suggesting a displacement of H5 toward the extracellular surface of the membrane. Since H5 and H6 contain cation-binding residues (*8*−*10*, *21*), the functional consequence of this movement is likely to be a change in the coordination of the bound cations. Therefore, although more subtle conformational changes should also occur to explain the various sequential steps observed in the enzyme catalytic cycle, the movement of the H5 helix appears critical for energy transduction by P-type ATPases.

Structural Model of TMs H5−*H6.* Homology modeling of the Na,K-ATPase based on the Ca-ATPase structure was performed to select the positions to be studied. To this end, we used Toyoshima et al. data of a Ca-bound enzyme likely in the E1 form (PDB 1EUL) (*11*). Two theoretical structures of the Ca-ATPase in a Ca-free conformation have been proposed: PDB 1FQU (Nakasako and Toyoshima) and 1KJU (*44*). However, these structures address structural changes in the cytoplasmic region of the enzyme rather than conformational transitions in the transmembrane region associated with ion transport. Thus, 1EUL coordinates for H5−H6 were not changed in PDB 1FQU and 1KJU. Consequently, we focused our modeling and hypothesis only in the information contained in PDB 1EUL.

Our findings, summarized in Table 2, correlate and validate the proposed structural model. For instance, Cys at positions predicted to be part of the extracellular joining loop appeared to be more accessible to the probes, while the modification of Cys residues close to the proposed borders of H5 (Ile^{787}Cys) and H6 (Thr^{797}Cys) better reflected the conformational changes in this region. The relatively weak modification of enzymes carrying replacements Thr^{781}Cys, Cys^{802} and Leu^{805}Cys suggests a narrow cation path along H4, H5,

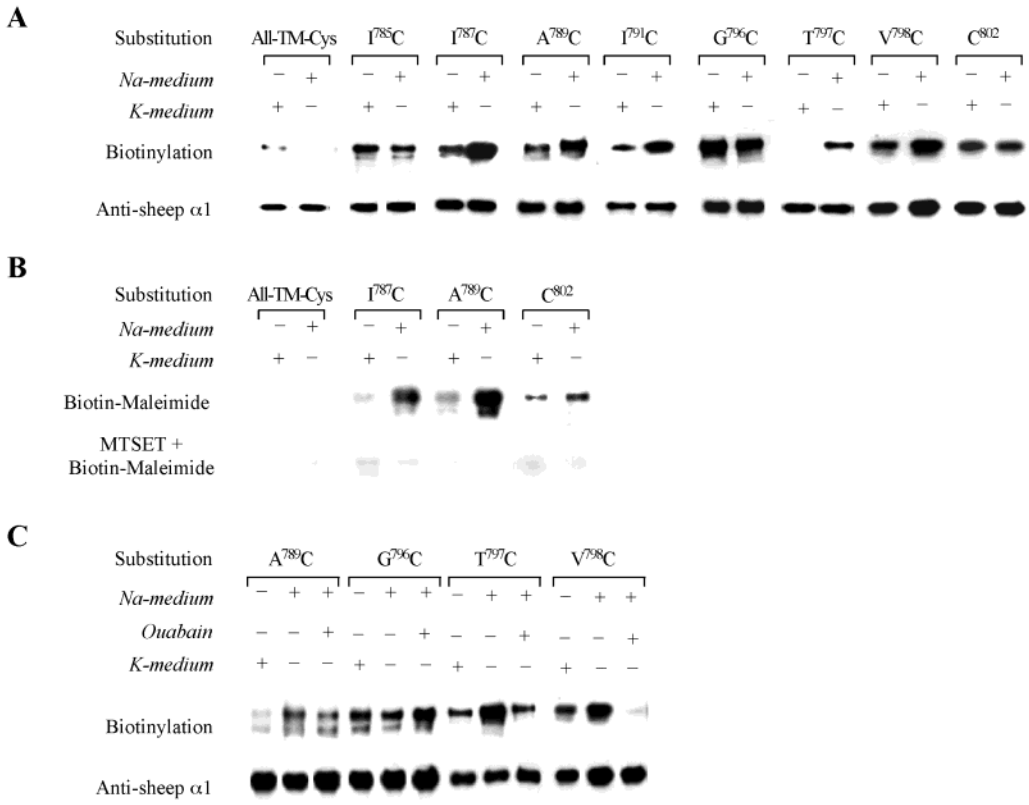

FIGURE 5: Biotinylation of Cys-substituted enzymes by treatment with biotin-maleimide. Blots were stained either with HRP-streptavidin to detect biotinylated proteins or with antibodies against sheep α1 subunit to verify similar levels of heterologous enzyme in each lane. (A) COS cells expressing the indicated enzyme were treated with 0.5 mM biotin-maleimide for 30 min in *K-medium* or *Na-medium*. (B) COS cells expressing the indicated enzyme were treated with 0.5 mM biotin-maleimide for 30 min after exposure to 5 mM MTSET for 30 s. (C) COS cells expressing the indicated enzyme were treated with biotin-maleimide for 30 min in *K-medium*, *Na-medium*, and *Na-medium* plus 2 mM ouabain.

Table 2: Summary of Relative Accessibility of Residues in the H5−H6 Loop[a]

	enzyme conformation with reagent					
	Hg^{2+}		MTSET		biotin-maleimide	
residue	E1	E2P	E1	E2P	E1	E2P
All-TM-Cys	−	−	−	−	−	−
$Thr^{781}Cys$	−	−	−	−	ND	ND
$Ile^{785}Cys$	−	−	−	+*	+	+
$Ile^{787}Cys$	+	++*	−	+*	+	++*
$Ala^{789}Cys$	+	+	+	+	+	++*
$Ile^{791}Cys$	+	+	−	−	−	+*
$Gly^{796}Cys$	+	+	+	+	+	+
$Thr^{797}Cys$	+	+	++	+++*	−	++*
$Val^{798}Cys$	+	+	+	+	+	++*
$Thr^{799}Cys$	−	−	−	−	ND	ND
Cys^{802}	−	−	−	−	±	±
$Leu^{805}Cys$	−	+*	−	−	ND	ND

[a] An asterisk indicates higher apparent reactivity when the enzyme is in the phosphorylated conformation. ND = not determined.

and H6. This appears to be in agreement with that observed in the Ca-ATPase structure (*11*) and suggested by studies where MTSEA or MTSET treatment did not affect enzymes carrying Cys introduced in H5 (*45*). Similarly, the poor modification of $Ile^{791}Cys$ by MTSET and biotin-maleimide suggests that the large H7−H8 joining loop covers part of the H5−H6 external loop. Also in agreement with the model is the protection of $Thr^{797}Cys$ and $Val^{798}Cys$ enzymes by the presence of ouabain in the biotin-maleimide treatment medium. Previous structure-function studies have shown the participation of Thr^{797} in ouabain binding (*25*).

Structure−Function Role of the S5H5 Helix. Cys introduced at several positions were consistently more reactive (as indicated by more extensive labeling or enzyme inhibition) when the enzyme was treated *Na-medium* than when it was treated in *K-medium*. *Na-medium* favors a phosphorylated form of the enzyme. The increased labeling of $Ala^{789}Cys$- or $Gly^{796}Cys$-replaced enzymes when treated in the presence of ouabain supports this observation, since the steroid stabilizes the phosphorylated form of the enzyme (*42*, *43*). Although alternative conformational changes (helix rotations etc.) might explain the larger accessibility of residues in H5−H6 when the enzyme is phosphorylated, the simplest interpretation of our results is the outward movement of H5 upon enzyme phosphorylation. In this direction, Kaplan and collaborators have shown that the H5−H6 hairpin appears to interact weakly with the surrounding TMs and it is released toward the extracellular side of the membrane when it is cleaved from the cytoplasmic loops (*23*, *24*). The outward movement of H5 also appears feasible considering the proximity of Asp^{369}, the phosphorylated amino acid, and Phe^{748}, the starting residue in the H5 helix. Accordingly, it is conceivable that a phosphorylation-induced short displacement of Asp^{369} into the protein core (i.e., toward the stalk region and away from the nucleotide-binding site) would project the S5H5 helix into the transmembrane domain. Such change in the disposition of H5 within the transmembrane region would have direct effects on the cation coordination. However, because of limitations of the experiments, it is not clear whether the movement of H5 is

associated with locking Na^+ in an occluded conformation or the release of Na^+ to the extracellular media. Similarly, our results do not exclude simultaneous neighboring conformational changes that might have contributed to a larger labeling of cysteines in the H5−H6 joining loop. Nevertheless, although additional structural data are required to establish other specific molecular events associated with cation translocation, the key role of H5 in energy transduction appears clear.

REFERENCES

1. Shull, G. E., Schwartz, A., and Lingrel, J. B. (1985) Amino acid sequence of the catalytic subunit of the (Na^+ + K^+)ATPase deduced from a complementary DNA. *Nature 316*, 691−695.
2. Glynn, I. (1985) The Na^+, K^+-transporting adenosine triphosphatase. in *Enzymes of Biological Membranes* (Martonosi, P. C., Ed.) pp 28−114, Plenum Press, New York.
3. Jørgensen, P. L., Nielsen, J. M., Rasmussen, J. H., and Pedersen, P. A. (1998) Structure−function relationships of E1−E2 transitions and cation binding in Na, K-pump protein. *Biochim. Biophys. Acta 1365*, 65−70.
4. Lutsenko, S., and Kaplan, J. H. (1995) Organization of P-type ATPases: significance of structural diversity. *Biochemistry 34*, 15607−15613.
5. Farley, R. A., Tran, C. M., Carilli, C. T., Hawke, D., and Shively, J. E. (1984) The amino acid sequence of a fluorescein-labeled peptide from the active site of (Na, K)-ATPase. *J. Biol. Chem. 259*, 9532−9535.
6. Lane, L. K., Feldmann, J. M., Flarsheim, C. E., and Rybczynski, C. L. (1993) Expression of rat α1 Na, K-ATPase containing substitutions of "essential" amino acids in the catalytic center. *J. Biol. Chem. 268*, 17930−17934.
7. Ohta, T., Nagano, K., and Yoshida, M. (1986) The active site structure of Na^+/K^+-transporting ATPase: location of the 5′-(p-fluorosulfonyl)benzoyladenosine binding site and soluble peptides released by trypsin. *Proc. Natl. Acad. Sci. U.S.A. 83*, 2071−2075.
8. Argüello, J. M., and Lingrel, J. B. (1995) Substitutions of serine 775 in the alpha subunit of the Na, K-ATPase selectively disrupt K^+ high affinity activation without affecting Na^+ interaction. *J. Biol. Chem. 270*, 22764−22771.
9. Argüello, J. M., Peluffo, R. D., Feng, J., Lingrel, J. B., and Berlin, J. R. (1996) Substitution of glutamic 779 with alanine in the Na, K-ATPase alpha subunit removes voltage dependence of ion transport. *J. Biol. Chem. 271*, 24610−24616.
10. Argüello, J. M., and Kaplan, J. H. (1994) Glutamate 779, an intramembrane carboxyl, is essential for monovalent cation binding by the Na, K-ATPase. *J. Biol. Chem. 269*, 6892−6899.
11. Toyoshima, C., Nakasako, M., Nomura, H., and Ogawa, H. (2000) Crystal structure of the calcium pump of sarcoplasmic reticulum at 2.6 Å resolution. *Nature 405*, 647−655.
12. Sweadner, K. J., and Donnet, C. (2001) Structural similarities of Na, K-ATPase and SERCA, the $Ca^{(2+)}$-ATPase of the sarcoplasmic reticulum. *Biochem. J. 356*, 685−704.
13. MacLennan, D. H., Brandl, C. J., Korczak, B., and Green, N. M. (1985) Amino acid sequence of a Ca^{2+} + Mg^{2+}-dependent ATPase from rabbit muscle sarcoplasmic reticulum, deduced from its complementary DNA sequence. *Nature 316*, 696−700.
14. Ambesi, A., Miranda, M., Allen, K. E., and Slayman, C. W. (2000) Stalk segment 4 of the yeast plasma membrane H^+-ATPase. Mutational evidence for a role in the E1-E2 conformational change. *J. Biol. Chem. 275*, 20545−20550.
15. Andersen, J. P., and Vilsen, B. (1993) Functional consequences of substitution of the seven-residue segment LysIleArgAspGlnMetAla240 located in the stalk helix S3 of the Ca^{2+}-ATPase of sarcoplasmic reticulum. *Biochemistry 32*, 10015−10020.
16. Soteropoulos, P., and Perlin, D. S. (1998) Genetic probing of the stalk segments associated with M2 and M3 of the plasma membrane H^+-ATPase from *Saccharomyces cerevisiae*. *J. Biol. Chem. 273*, 26426−26431.
17. Soteropoulos, P., Valiakhmetov, A., Kashiwazaki, R., and Perlin, D. S. (2001) Helical stalk segments S4 and S5 of the plasma membrane H^+-ATPase from *Saccharomyces cerevisiae* are optimized to impact catalytic site environment. *J. Biol. Chem. 276*, 16265−16270.
18. McIntosh, D. B. (2000) Portrait of a P-type pump. *Nat. Struct. Biol. 7*, 532−535.
19. Argüello, J. M., Whitis, J., Cheung, M. C., and Lingrel, J. B. (1999) Functional role of oxygen-containing residues in the fifth transmembrane segment of the Na, K-ATPase alpha subunit. *Arch. Biochem. Biophys. 364*, 254−263.
20. Vilsen, B., and Andersen, J. P. (1998) Mutation to the glutamate in the fourth membrane segment of Na^+, K^+-ATPase and Ca^{2+}-ATPase affects cation binding from both sides of the membrane and destabilizes the occluded enzyme forms. *Biochemistry 37*, 10961−10971.
21. Kuntzweiler, T. A., Argüello, J. M., and Lingrel, J. B. (1996) Asp804 and Asp808 in the transmembrane domain of the Na, K-ATPase alpha subunit are cation coordinating residues. *J. Biol. Chem. 271*, 29682−29687.
22. Argüello, J. M., and Kaplan, J. H. (1991) Evidence for essential carboxyls in the cation-binding domain of the Na, K-ATPase. *J. Biol. Chem. 266*, 14627−14635.
23. Lutsenko, S., Anderko, R., and Kaplan, J. H. (1995) Membrane disposition of the M5-M6 hairpin of the Na, K-ATPase α subunit is ligand dependent. *Proc. Natl. Acad. Sci. U.S.A. 87*, 4566−4570.
24. Gatto, C., Lutsenko, S., Shin, J. M., Sachs, G., and Kaplan, J. H. (1999) Stabilization of the H, K-ATPase M5M6 membrane hairpin by K^+ ions. Mechanistic significance for P2-type ATPases. *J. Biol. Chem. 274*, 13737−13740.
25. Feng, J., and Lingrel, J. B. (1994) Analysis of amino acid residues in the H5−H6 transmembrane and extracellular domains of Na, K-ATPase alpha subunit identifies threonine 797 as a determinant of ouabain sensitivity. *Biochemistry 33*, 4218−4224.
26. Palasis, M., Kuntzweiler, T. A., Argüello, J. M., and Lingrel, J. B. (1996) Ouabain interactions with the H5−H6 hairpin of the Na, K-ATPase reveal a possible inhibition mechanism via the cation binding domain. *J. Biol. Chem. 271*, 14176−14182.
27. Price, E. M., and Lingrel, J. B. (1988) Structure−function relationships in the Na, K-ATPase alpha subunit: site-directed mutagenesis of glutamine-111 to arginine and asparagine-122 to aspartic acid generates a ouabain-resistant enzyme. *Biochemistry 27*, 8400−8408.
28. Zichittella, A. E., Shi, H. L., and Argüello, J. M. (1999) Reactivity of cysteines in the transmembrane region of the Na, K-ATPase α subunit probed with Hg^{2+}. *J. Membr. Biol. 177*, 187−197.
29. Shi, H. G., Mikhaylova, L., Zichittella, A. E., and Argüello, J. M. (2000) Functional role of cysteine residues in the Na, K-ATPase α subunit. *Biochim. Biophys. Acta 1464*, 177−187.
30. Sarkar, G., and Sommer, S. S. (1990) The "megaprimer" method of site-directed mutagenesis. *BioTechniques 8*, 404−407.
31. Jewell, E. A., and Lingrel, J. B. (1991) Comparison of the substrate dependence properties of the rat Na, K-ATPase alpha 1, alpha 2, and alpha 3 isoforms expressed in HeLa cells. *J. Biol. Chem. 266*, 16925−16930.
32. Bradford, M. M. (1976) A rapid and sensitive method for the quantitation of microgram quantities of protein utilizing the principle of protein-dye binding. *Anal. Biochem. 72*, 248−254.
33. Munzer, J. S., Daly, S. E., Jewell Motz, E. A., Lingrel, J. B., and Blostein, R. (1994) Tissue- and isoform-specific kinetic behavior of the Na, K-ATPase. *J. Biol. Chem. 269*, 16668−16676.
34. Efendiev, R., Bertorello, A. M., Pressley, T. A., Rousselot, M., Feraille, E., and Pedemonte, C. H. (2000) Simultaneous phosphorylation of Ser11 and Ser18 in the alpha-subunit promotes the recruitment of Na^+, K^+-ATPase molecules to the plasma membrane. *Biochemistry 39*, 9884−9892.
35. Schägger, H., and von Jagow, G. (1987) Tricine-sodium dodecyl sulfate-polyacrylamide gel electrophoresis for the separation of proteins in the range of 1 to 10 kDa. *Anal. Biochem. 166*, 368−379.
36. Guex, N., and Peitsch, M. C. (1997) SWISS-MODEL and the Swiss-PdbViewer: an environment for comparative protein modeling. *Electrophoresis 18*, 2714−2723.
37. Garrahan, P. J., and Glynn, I. M. (1967) The sensitivity of the sodium pump to external sodium. *J. Physiol. (London) 192*, 175−188.
38. Garrahan, P. J., and Glynn, I. M. (1967) The behavior of the sodium pump in red cells in the absence of external potassium. *J. Physiol. (London) 192*, 159−174.
39. Heyse, S., Wuddel, I., Apell, H. J., and Stürmer, W. (1994) Partial reactions of the Na, K-ATPase: Determination of rate constants. *J. Gen. Physiol. 104*, 197−240.

40. Beaugé, L. A., and Glynn, I. M. (1979) Sodium ions, acting at high-affinity extracellular sites, inhibit sodium-ATPase activity of the sodium pump by slowing dephosphorylation. *J. Physiol. (London) 289*, 17−31.
41. Hansen, O. (1984) Interaction of cardiac glycosides with ($Na^+ + K^+$)-activated ATPase. A biochemical link to digitalis-induced inotropy. *Pharmacol. Rev. 36*, 143−163.
42. Yoda, A., and Yoda, S. (1982) Interaction between ouabain and the phosphorylated intermediate of Na, K-ATPase. *Mol. Pharmacol. 22*, 700−705.
43. Wallick, E. T., and Schwartz, A. (1988) Interaction of cardiac glycosides with Na^+, K^+-ATPase. *Methods Enzymol. 156*, 201−213.
44. Xu, C., Rice, W. J., He, W., and Stokes, D. L. (2002) A structural model for the catalytic cycle of Ca(2+)-ATPase. *J. Mol. Biol. 316*, 201−211.
45. Guennoun, S., and Horisberger, J. D. (2000) Structure of the 5^{th} transmembrane segment of the Na, K-ATPase alpha subunit: a cysteine-scanning mutagenesis study. *FEBS Lett. 482*, 144−148.

BI025721K